ISSN 0915-6364

NATIONAL INSTITUTE FOR FUSION SCIENCE

Dielectronic Recombination Rate Coefficients to Excited States of *He* from He^+

J.G. Wang, T. Kato and I. Murakami

(Received - Mar. 2, 1999)

NIFS-DATA-53 Apr. 1999

RESEARCH REPORT
NIFS-DATA Series

NAGOYA, JAPAN

Dielectronic recombination rate coefficients to excited states of He from He^+

J.G. Wang, T. Kato, and I. Murakami

National Institute for Fusion Science 322-6 Oroshi-cho, Toki-shi 509-5292, Japan

A Simplified Relativistic Configuration Interaction (SRCI) method is used to calculate the dielectronic recombination rate coefficients to the excited states of He from He^+. In this method, the infinite resonant doubly excited states involving high Rydberg states are treated conveniently in a unified mannar by interpolation. The dielectronic recombination processes for $\Delta N = 1$ and $\Delta N = 2$ transitions are included in our calculations, and the cross sections are in agreements with the experimental measurements. The rate coefficients to the excited states are fitted to an analytical formula and the n-dependences of the fitting parameters are discussed.

Keyword: simplified relativistic configuration interaction method, dielectronic recombination rate coefficients, excited states of He, an analytical formula

1. Introduction

Dielectronic Recombination (DR) can be regarded as a resonant radiative recombination process. As a free electron with a specific kinetic energy collides with an ion A^{q+}, one of the bound electrons of the ion A^{q+} is excited from the initial $n_a l_a$ orbital into the $n_r l_r$ orbital, the free electron is then captured into an unoccupied orbital nl and forms a resonant doubly excited state; subsequently, the resonant doubly excited state decays into a non-autoionizing state through radiative transition processes. Its importance to influence the ionic balance in high temperature plasmas, such as solar corona, has been known for many years [1]. Its radiative emission is a significant contributor for plasma cooling in hot plasmas in fusion experiments. The dielectronic satellites of hydrogen-like ion have also been used to measure plasma densities in high density plasmas [2] and the electron temperatures in solar flares [3, 4, 5].

Many theoretical methods have been developed to calculate the DR process[6, 7, 8, 9]. In these calculations, it is a tedious work to obtain the accurate DR rate coefficients since they involve many resonant doubly excited high Rydberg states. Due to the difficulty of numerical calculation on wavefunction and too enormous number of high Rydberg states, most calculations either neglect high-lying doubly excited states or simply use the n^{-3} scaling law to treat them[10, 11, 12, 13]. In fact, Quantum Defect Theory (QDT) has been developed to treat the atomic processes involving high Rydberg states[14, 15, 16], which was also used to study the DR cross sections and rate coefficients for high Rydberg states by extrapolation[17, 18, 19, 20]. Recently, in the frame of QDT, we have developed a Simplified Relativistic Configuration Interaction (SRCI) method to study the dielectronic recombination processes[21, 22, 23, 24]. In this method, all the resonant doubly excited high Rydberg states are classified into different channels with same angular momentum quantum number and same angular momentum coupling type. In each channel, the defined energy-normalized matrix elements vary smoothly with the energy of high Rydberg states. Only a few points (including a continuum point) are calculated, the many resonant high Rydberg states can be treated in an unified manner by interpolation (rather than extrapolation), and then the DR cross sections and rate coefficients can be obtained conveniently.

Helium is one of the most common species in laboratory and astrophysical plasmas. It played an important role in the development of plasma spectroscopy and spectroscopic diagnostics. Helium is also the ion with lowest atomic number which DR is possible, compared to the eletron-nucleus interaction between the free eletron and ion, the relative strength of electron-electron interaction (which mediates the DR process) is larger for Helium than any other ion. This fact makes the calculation of DR more difficult for helium. We have calculated the DR processes of helium for $\Delta N = 1$ transitions [21], and the results are in good agreement with the absolute cross section measurements within 10%. In present paper, we calculate the DR processes of helium for $\Delta N = 2$ transitions, and the cross sections are compared with the experimental measurements[25]. As is known for us, the past thereotical and experimental works on DR of He^+ are focused on the total dielectronic recombination rate coefficients or corss sections [1, 17, 21, 25, 26, 27, 28, 29, 30, 31]. But now, if individual line intesities have to be evaluated for the plasma cooling or spectroscopic diagnostic, the partial DR rate coefficients to the excited states must be known. So we

calculate the partial DR rate coefficients to the excited states of He from He^+, and then for applied convenience, the rate coefficients are fitted to an analytical formula and the n-dependence of the fitting parameters are discussed.

2. Theoretical Method

The DR process of he^+ has the form

$$e^- + He^+(n_a l_a) \rightarrow He(n_r l_r nl)^{**} \rightarrow He(n_k l_k)^* + h\nu. \quad (1)$$

here, when $n_r - n_a = 1$, the process is called DR for $\Delta N = 1$ transition, which is according to $2l_r nl(n \geq 2)$ resonances; when $n_r - n_a = 2$, the process is called DR for $\Delta N = 2$ transition, which is according to $3l_r nl(n \geq 3)$ resonances. For the DR processes of $\Delta N = 2$, there exist new Auger processes to $He^+(2s)$ and $He^+(2p)$ besides $He^+(1s)$. This will increase the complexity of calculation.

The cross section of resonant capture processes, in which the He^+ ion in initial state $i(n_a l_a)$ captures a free electron with a specific energy ϵ_i and forms the He atom in the resonant doubly excited state $j(n_r l_r nl)$, can be treated in the isolated resonance approximation (atomic unit is used throughout unless specified),

$$\sigma^c_{ij} = \frac{\pi^2\hbar^3}{m_e\epsilon_i}\frac{g_j}{2g_i}A^a_{ji}\cdot\delta(\epsilon-\epsilon_i), \quad (2)$$

where g_i and g_j are the statistical weight of the state i and j,respectively. A^a_{ji} is Auger decay rate (inverse resonant capture), which can be calculated by Fermi golden rule,

$$A^a_{ji} = \frac{2\pi}{\hbar}|<\Psi_j|\sum_{s<t}\frac{1}{r_{s,t}}|\Psi_{i\epsilon_i}>|^2, \quad (3)$$

where Ψ_j and $\Psi_{i\epsilon_i}$ are antisymmetrized many-electron wavefunctions for j state and i state plus a free electron, respectively.

We construct the configuration wavefunctions $\phi(\Gamma JM)$ (Γ denotes the configuration $2n_r l_r nl$ and parity) as antisymmetrized product-type wavefunctions from central-field Dirac orbitals with appropriate angular momentum coupling[32]. All relativistic single-electron wavefunctions (bound and continuum) are calculated based on the atomic self-consistent potential [33, 34]. An atomic state function for the state $j(n_r l_r nl)$ with total angular momentum JM is then expressed as linear expansion of the configuration wavefunctions with same principal quantum numbers (n_r, n), and same orbital angular momentum quantum numbers (l_r, l)

$$\psi_j(JM) = \sum_{\lambda=1}^{m} C_{j\lambda}\phi(\Gamma_\lambda JM). \quad (4)$$

Here m is the number of the configuration wavefunctions and the mixing coefficients $C_{j\lambda}$ for state j are obtained by diagonalizing the relevant Hamiltonian matrices[32]. The free state is chosen as the single configuration wavefunction. Then we have

$$A^a_{ji} = \frac{2\pi}{\hbar}|\sum_{\lambda=1}^{m} C_{j\lambda}M^a_{ij\lambda}|^2, \quad (5)$$

where the Auger decay matrix element $M^a_{ij\lambda}$ is defined as

$$M^a_{ij\lambda} = <\phi(\Gamma_\lambda JM)|\sum_{s<t}\frac{1}{r_{s,t}}|\Psi_{i\epsilon_i}>. \quad (6)$$

Based on QDT, when l are fixed and n varies from bound to continuum state, all the resonant doubly excited states with same J will form a channel. In the channel, the energy-normalized matrix element can be defined as

$$\overline{M}^a_{ij} = \sum_{\lambda=1}^{m} C_{j\lambda}M^a_{ij\lambda}\cdot(\nu_n^{3/2}/q), \quad (7)$$

here (ν_n^3/q^2) is the density of state, $\nu_n = n - \mu_n$, and μ_n is the corresponding quantum defect. This energy-normalized matrix element $\overline{M}^a_{ij}$ varies smoothly with the electron orbital energy in the channel[21, 23]. When the energy-normalized matrix elements of a few states (including one continuum state) in a channel have been calculated, the Auger decay matrix elements of infinite discrete states of that channel can be obtained by interpolation. From the expression (9) and (7), the Auger rates and capture rates (by detailed balance) of the infinite resonant doubly excited states can be calculated conveniently.

The resonant doubly excited state may autoionize with a rate A^a_{ji} by reemitting Auger electron or decay radiately into a lower energy state k with a radiative rate A^r_{jk}, which is defined as

$$A^r_{jk} = \frac{4e^2\omega}{3\hbar c^3 g_j}|<\Psi_j|T^{(1)}|\Psi_k>|^2, \quad (8)$$

where ω is photon energy, $T^{(1)}$ is electronic dipole operator [21]. The atomic wavefunction Ψ_k for final state k can be constructed in the similar way as the expression (4)

$$\psi_k(J'M') = \sum_{\lambda'=1}^{m'} C_{k\lambda'}\phi'(\Gamma'_{\lambda'}J'M'). \quad (9)$$

Then we have

$$A^r_{jk} = \frac{4e^2\omega}{3\hbar c^3 g_j}|\sum_{\lambda,\lambda'=1}^{m,m'} C_{j\lambda}C_{k\lambda'}M^T_{\lambda,\lambda' jk}|^2, \quad (10)$$

where the radiative transition matrix element is defined as

$$M^T_{\lambda,\lambda' jk} = <\phi(\Gamma_\lambda JM)|T^{(1)}|\phi'(\Gamma'_{\lambda'}J'M')>. \quad (11)$$

For the radiative process with certain final state $k(1sn_k l_k$ the resonant doubly excited states with the fixed (l) and

different orbital energy form a channel. In the channel, the energy-normalized radiative transition matrix element is defined as

$$\overline{M^r_{jk}} = \sum_{\lambda,\lambda'=1}^{m,m'} C_{j\lambda} C_{k\lambda'} M^r_{\lambda,\lambda' jk} \cdot (\nu_n^{3/2}/q). \quad (12)$$

This energy-normalized matrix element varies slowly with the electron orbital energy[21, 35, 36, 37]. By interpolation, all the energy-normalized matrix elements of infinite discrete states in a channel can be obtained. From the expression (12), we can obtain all the radiative rates in the channel.

The resonance energy ϵ_i can be calculated under the frozen core approximation [38]. Then, we can obtain the DR cross sections for any resonant doubly excited states conveniently,

$$\sigma_{ij;k} = \frac{\pi^2\hbar^3}{m_e\epsilon_i}\frac{g_j}{2g_i}\frac{A^a_{ji}A^r_{jk}}{\sum_{k'}A^r_{jk'} + \sum_{i'}A^a_{ji'}} \cdot \delta(\epsilon - \epsilon_i) \quad (13)$$

Here the summation i' is over all possible states of He^+ ion, and the summation k' is over all possible states of He whose energy are below state j.

The summation of cross sections over all possible k is expressed as

$$\sigma_{ij} = \sum_k \sigma_{ij;k}. \quad (14)$$

The DR strength, which is the integral of the DR cross section over the natural width of the resonance, can be written as

$$S_{ij} = \frac{\pi^2\hbar^3}{m_e\epsilon_j}\frac{g_j}{2g_i}\frac{A^a_{ji}\sum_k A^r_{jk}}{\sum_{k'}A^r_{jk'} + \sum_{i'}A^a_{ji'}}. \quad (15)$$

We assume that the velocity distribution of the free electron as the Maxwell–Boltzmann distribution, then the dielectronic recombination rate coefficients can be express as

$$\alpha_{ij;k} = \left(\frac{2\pi\hbar^2}{m_e\kappa T}\right)^{3/2} e^{-\frac{\epsilon_j}{\kappa T}}\frac{g_j}{2g_i}\frac{A^a_{ji}A^r_{jk}}{\sum_{k'}A^r_{jk'} + \sum_{i'}A^a_{ji'}} \quad (16)$$

where T is the temperature of the electron, κ is Boltzmann constant. The partial dielectronic recombination rate coefficients to excited state k can be express as

$$\alpha^{DR}(k) = \sum_j \alpha_{ij;k}, \quad (17)$$

Here, the summation of j includes all the resonant doubly excited states. The total dielectronic recombination rate can be express as

$$\alpha^{DR} = \sum_{j,k} \alpha_{ij;k} \quad (18)$$

3. Result and Discussion

There are enormous intermediate resonance states involved in the DR process, which makes the explicit calculations not practicable. Hence, the n^{-3} scaling law is widely used in the literature to extrapolate the satellite intensity factors (proportional to DR cross section) for higher ($n \geq 4$) resonances[10, 11, 12]. Based on QDT, we have developed the SRCI method, in which all the high-lying resonant doubly excited states are treated conveniently through interpolation. In present paper, we study the dielectronic recombination processes of He from He^+, and obtain the cross sections and rate coefficients to excited states.

In the previous paper[21], we have calculated the DR cross sections of helium for $\Delta N = 1$ transitions, and the results are in good agreement with the absolute measurements[31] within 10%. This shows that our SRCI method has included the main part of the correlation, and it can satisfy the need for relevant applications. In present paper, in order to calculate the rate coefficients, we also include the DR processes of helium for $\Delta N = 2$ transitions. The DR processes through the $\Delta n = 2$ resonance states are more challenging theoretically because the electron-electron interaction is expect to be stronger than through the $\Delta n = 1$ resonance states, and meantimes for these $\Delta n = 2$ resonance states, there are more Auger channel, while only one contributes to the capture processes. Our convoluted cross sections are compared with the experimental measurements[25], as shown in Fig.1. In the convolution, we only include the doubly excited states $3l_r nl$ with $3 \leq n \leq 6$. The thereotical peaks for $n = 3$ and $n = 4$ show a good agreements with experimental measurements. But the thereotical peaks for $n = 5$ and $n = 6$ are higher than experimental measurements. This is because the contributions of high-n resonaces with $n \geq 5$ haven't been fully included in the experimets due to field ionization effects[31, 25]. Meanwhile, the contributions of high-n resonaces with $n \geq 7$ are observed partially in the experiments, which are located in the higher energy range than our thereotical value in Fig.1. We also find that the main contributions to cross sections come from the $3pnd$ resonances[25]. In the calculation on rate coefficients, the contributions of all high-n resonances are included.

Using eq.(17) and eq.(18), we can calculate rate coefficients to excited states and total rate coefficients. The total rate coefficients are plotted in Fig.2. It can be seen that the main contributions to rate coefficients come from the $2l_r nl$ resonances, and the contributions from $3l_r nl$ resonances are lower than 10%. For $2l_r nl$ resonances, there is only one Auger channel to $He^+(1s)$, whose inversion processes are the capture processes. However, for $3l_r nl$ resonances, besides Auger channel to $He^+(1s)$ involving the capture processes, there are Auger channels to to $He^+(2s)$ and $He^+(2p)$, especially, the Auger rates to $He^+(2s)$ and $He^+(2p)$ are much larger than the Auger rates to $He^+(1s)$. From eq.(16), we can conclude that the rate coefficients for $2l_r nl$ resonances will be much larger than $3l_r nl$ resonances.

The rate coefficients to excited states are shown in

Fig.3, Fig.4 and Fig.5 . In Fig.3(a) and (b), we plot the rate coefficients to final states $1sns(n^1S)$ and $1sns(n^3S)(n = 2-100)$. For $n = 3-100$, the rate coefficients come from the according doubly excited states $2pns(n = 3-100)$ by radiative transition $2pns \rightarrow 1sns$, and decrease with increasing n; for $n = 2$, there are many other transitions $2snp \rightarrow 1s2s(n = 3-\infty)$ contributing to the rate coefficients, besides the transition $2p2s \rightarrow 1s2s$. So the rate coefficients to final states $1s2s$ are much larger than others, as shown in Fig.3(a) and Fig.3(b). For the final states $1s2p(2^1P)$, it comes from the transitions $2p^2 \rightarrow 1s2p$ and $2pnp \rightarrow 1s2p(n = 3-\infty)$, which is larger than $1snp(n^1P)(n = 3-100)$, as shown as Fig.3(c). For the final states $1s2p(2^3P)$, it is well known that configuration $2p^2$ can forms terms 2^1S, 2^1D and 2^3P. According to the selection rule of dipole transitions, only 2^3P can contribute to the final states $1s2p(2^3P)$. However, the Auger rates of $2p^2(2^3P)$ are many magnitudes smaller than $2p^2(2^1S)$ and $2p^2(2^1D)$, which causes a very small cross section for $2p^2(2^3P)$ resonance [31, 25, 21], so the contributions to the final states $1s2p(2^3P)$ don't come from $2p^2$ configuration but from the doubly excited states $2pnp(n \geq 3)$ by transitions $2pnp \rightarrow 1s2p$. This causes the rate coefficients to final states $1s2p(2^3P)$ smaller than the rate coefficients to $1s3p(2^3P)$, which come from the transition $2p3p \rightarrow 1s3p$. Comparing Fig.3(a), Fig.3(b), Fig.3(c) and Fig.3(d), we can found the curves of rate coefficients are much closer for different final states n in Fig.3(a) and Fig.3(c). This is because the doubly excited states (such as $2pns^1P$ and $2pnp^1D$), which is the main contributor to the final states in Fig.3(a) and Fig.3(c), have very large Auger rate A^a. Using eq.(16), if $A^a \gg A^r$, $\alpha \propto \frac{A^a_{ji}\sum_k A^r_{jk}}{\sum_{k'} A^r_{jk'}+\sum_{i'} A^a_{ji'}} \sim \sum_k A^r_{jk}$. Here, the principal radiative processes are $2p \rightarrow 1s$, which are almost independent on n. So the rate coefficients vary slowly with n. But for the final states in Fig.3(b) and Fig.3(d), the A^a of the involved doubly excited states is not very large and the curves are not so close with increasing n. In Fig.4 and Fig.5, we plot the rate coefficients to final states $1snd(n^1D, n^3D)$, $1snf(n^1F, n^3F)$, $1sng(n^1G, n^3G)$, and $1snh(n^1H, n^3H)$. The rate coefficients in Fig.5 are two magnitudes smaller than Fig.4. As l increases, the Auger rates for the doubly excited states $He^{**}(2l_rnl)$ decreases very fast. When $l = 4, 5$ in Fig.5, $A^a \ll A^r$, and then $\alpha \propto \frac{A^a_{ji}\sum_k A^r_{jk}}{\sum_{k'} A^r_{jk'}+\sum_{i'} A^a_{ji'}} \sim A^a_{ji}$. so the small rate coefficients in Fig.5 are the direct results of very small Auger rates in the involved doubly excited states.

In order to use the rate coefficients conveniently, we fit them into a formula with two fitting parameters as following:

$$\alpha_{fit} = 6.68167 \times 10^{-13}(\kappa T)^{-3/2} \cdot E_{av} \cdot S_t \cdot e^{-\frac{E_{av}}{\kappa T}} \quad (19)$$

Here, the fitting parameters E_{av} and S_t are according to the average incident electron energy and total integrated cross sections, respectively. The units of α_{fit}, κT, E_{av} and S_t are $cm^3 \cdot s^{-1}$, eV, eV and $10^{-20} cm^2 \cdot eV$, respectively. The fitting parameters are plotted in Fig.6-Fig.11. As we have mentioned above, when $n = 2$, the parameters S_t, which determine the rate coefficients directly, are larger than that when $n = 3$ for the final states $1sns$ (n^1S, n^3S) and $1snp$ (n^1P), and smaller than that when $n = 3$ for the final states $1snp$ (n^3P) as shown in Fig.6. The main contributions to $1s2p$ (n^3P) come from the transitons $2pnp \rightarrow 1s2p(n \geq 3)$, so the parameter E_{av} for $1s2p$ (2^3P) is larger than that for $1s2s$ $(2^1S, 2^3S)$ and $1s2p$ (2^1P), as shown in Fig.7.

With increasing n in $1sns$ (n^1S), the curve varies very slowly when $n < 20$, and decrease linearly when $n > 40$, as shown in Fig.6. As we have mentioned above, when $n < 20$, $A^a \gg A^r$, and then the integrated cross sections $S_{ij} \propto \frac{A^a_{ji}\sum_k A^r_{jk}}{\sum_{k'} A^r_{jk'}+\sum_{i'} A^a_{ji'}} \sim \sum_k A^r_{jk}$. Here, the principal radiative processes are $2p \rightarrow 1s$, which are almost independent on n. So the fitting integrated cross sections vary slowly with n. With increasing n, the A^a decreases as n^{-3} scaling law. When $n > 40$, $A^a \ll A^r$, and then $S_{ij} \propto \frac{A^a_{ji}\sum_k A^r_{jk}}{\sum_{k'} A^r_{jk'}+\sum_{i'} A^a_{ji'}} \sim A^a_{ji}$. So the fitting integrated cross sections decrease as n^{-3} scaling law with increasing n, and the curve in Fig.6 decrease linearly. With the increasing l in the final states $1snl$, the Auger rates of the involved doubly excited states become small, so the fitting integrated cross sections behave as n^{-3} scaling law in the final states with lower n, as shown in Fig.8 and Fig.10. Due to small integrated cross sections for $3l_rnl$ resonances, its effects on rate coefficients to excited states are not large, except the final states $1snd(n^1D, n^3D)$ originating from doubly excited states $3pnd$, as we have mentioned above. So the fitting elctron energies for final states $1snd(n^1D, n^3D)$ are higher than other final states, as shown as in Fig.9, Fig.7 and Fig.11. We aslo check the validity of fitting formula, and found that it is in good agreements with our numerical calculations with 3%, as an example shown in Fig.3(a) and Fig.3(c).

4. Conclusion

A simplified relativistic configuration interaction method is used to study the dielectronic recombination processes to excited states of helium. In this method, the infinite resonant doubly excited states involving high Rydberg state can be treated conveniently in a unified mannar by interpolation.The dielectronic recombination processes for $\Delta N = 1$ and $\Delta N = 2$ transitions are included in our calculations. In a previous paper, We have compared our calculated cross sections with the absolute measurements for $\Delta N = 1$ transitions [21]. In present paper, We have also compared our calculated cross sections with the absolute measurements for $\Delta N = 2$ transitions. The agreements of our calculation with the experimental measurements show that our SRCI method has included the main part of the correlation, and it can satisfy the need for relevant applications. The rate coefficients to the excited states are also fitted to an analytical formula and the n-dependences of the fitting parameters are discussed, which will be very convenient for the application in plasma physics.

This work was partily supported by the Japan Sociaty for Promotion of Science.

References

[1] A. Burgess, Astrophys. J. **139**, 776(1964);

[2] A. V. Vinogradov, I. Yu. Skobelev and E. A. Yukov, Sov. Phys. JETP **45**, 925 (1977).

[3] J. Dubau, A. H. Gabriel, M. Loulergue. L. Steenman-Clark and S. Volone, Mon. Not. R. Astr. Soc **195**, 705(1981).

[4] T. Kato, Physica Scripta **T73**,98(1997).

[5] T. Kato, T. Fujiwara, and Y. Hanaoka, Astrophys. J. **492**, 822(1998).

[6] W. Eissner and M. J. Seaton, J. Phys. B **6**, 2187(1972).

[7] H. E. Saraph and M. J. Seaton, Phil. Trans. Roy. Soc., **A271**, 1(1971).

[8] Y. Hahn, Phys. Rev. A **22**, 2896(1980).

[9] M. H. Chen, Phys. Rev. A **31**, 1449(1985).

[10] D. J. McLaughlin and Y. Hahn, Phys. Rev. A **29**, 712(1984).

[11] e.g. M. H. Chen, Phys. Rev. A **33**, 994(1986). J. Dubau, A.H.Gabriel, M.Loulergue, L.Steennan-Clark, S.Volonte, Mon. Not.. R. ast. Soc **195**, 705(1981).

[12] K. R. Karim and C. P. Bhalla, Phys. Rev. A **37**, 2599(1988).

[13] J. Nilson, J. Quant Spectras. Radiat Transfer **36**, 539(1986).

[14] M. Gailitis, Sov.Phys.-JETP **17**,1328 (1963).

[15] U. Fano, J. Opt. Soc. Am. **65**,979(1975).

[16] M.J. Seaton, Proc. Phys. Soc. Lond.,**88**,801(1966); Rep. Prog. Phys.,**46**,167(1983).

[17] J. Dubau, Ph. D. Thesis, 1973, University of London.

[18] M.J. Seaton and P.J. Storey, 1976,in Atomic processes and applications, edited by P.G. Burke and B.L. Moiseiwitsch, p.133(North-Holland Publishing Company).

[19] J. Dubau and S. Volonte, Rep. Prog. Phys.,**43**,167(1980).

[20] R.H. Bell and M.J. Seaton, J. Phys. B: At.Mol.Phys. bf 18,1589(1985).

[21] Jian-Guo Wang, Yi-Zhi Qu and Jia-Ming Li, Phys. Rev. A **52**, 4274(1995).

[22] Jian-Guo Wang, Yu Zou, Chen-Zhong Dong and Jia-Ming Li, Chin. Phys. Lett. **12**, 530(1995).

[23] Chen-zhong Dong, Yu Zou, Jian-Guo Wang and Jia-Ming Li, Acta Phys. Sin. **44**, 1712(1995).

[24] Yi-Zhi Qu, Jian-Guo Wang, Jian-Kui Yuan and Jia-Ming Li, Phys. Rev. A **57**, 1033 (1998).

[25] D. R. Dewitt, E. Lindroth, R. Schurch, H. Gao, T. Quinteros, and W. Zong, J. Phys. B: At. Mol. Opt. Phys. 28, L147(1995).

[26] T. Fujimoto, T. Kato, and Y. Nakamura, IPPJ-AM-23, 1982.

[27] A. Wolf, J. Berger, M. Bock, D. Habs, et al, Z. Phys. D 21, 69(1991).

[28] J. A. Tanis, E. M. Bernstain, S. Chantrenne, M. W. Clark,et al, Nucl. Instrum. Methods B 56/57, 337(1991).

[29] T. Tanabe, M. Tomizawa, K. Chida, T. Watanabe, et al, Phys. Rev. A 45, 276(1992).

[30] R. R. Harr, J. A. Tanis, V. L. Plano, K. E. Zaharakis, et al, Phys. Rev. A 47, R3472(1993).

[31] D. R. DeWitt, R. Schuch, T. Quinteros, H. Gao, W. Zong, H. Danared, M. pajek and N. R. Badnell, Phys. Rev. A50(1994) 1257.

[32] Zhong-Xin Zhao and Jia-Ming Li, Acta Phys. Sin. **34**, 1469(1985).

[33] Jia-Ming Li and Zhong-Xing Zhao, Acta Phys. Sini. **31**, 97(1982).

[34] D. A. Liberman, D. T. Cromer and J. T. Waber, Comput. Phys. Commun. **2**, 107(1971).

[35] Lei Liu and Jia-Ming Li, Acta Phys. Sin. **42**, 1901(1993).

[36] Jian-Guo Wang, Xiao-Ming Tong and Jia-Ming Li, Acta Phys. Sin. **45**, 13(1996), see also Yi-Zhi Qu, Jian-Guo Wang, and Jia-Ming Li, Acta Phys. Sin. **46**, 249(1997).

[37] Cheng Zhu, Jian-Guo Wang, Yi-Zhi Qu and Jia-Ming Li, Phys. Rev. A **57**, 1747(1998).

[38] C. M. Lee (Jia-Ming Li), Phys. Rev. A **10**, 584(1974).

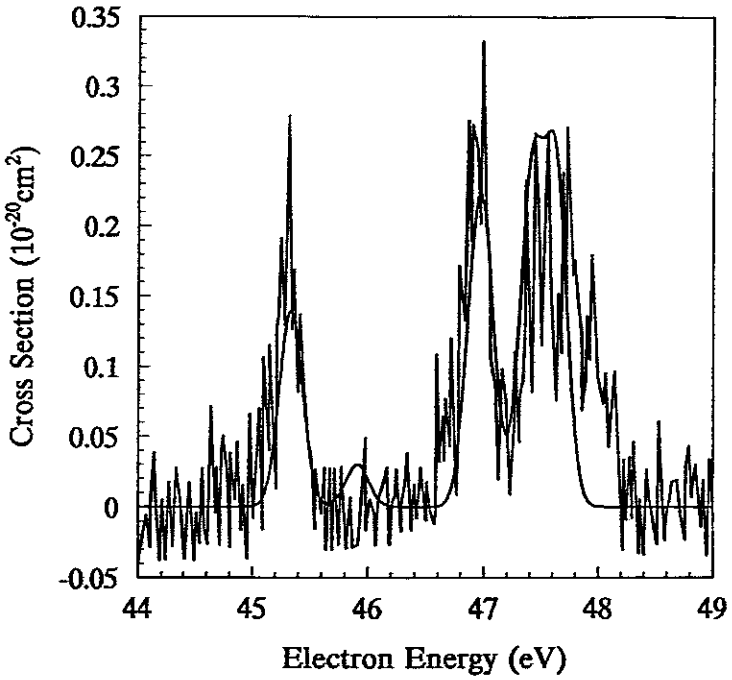

Fig.1 DR cross section for the $\Delta n = 2$ resonances. Solid line: Present theoretical results; Gray line: Experimental measurements[25]

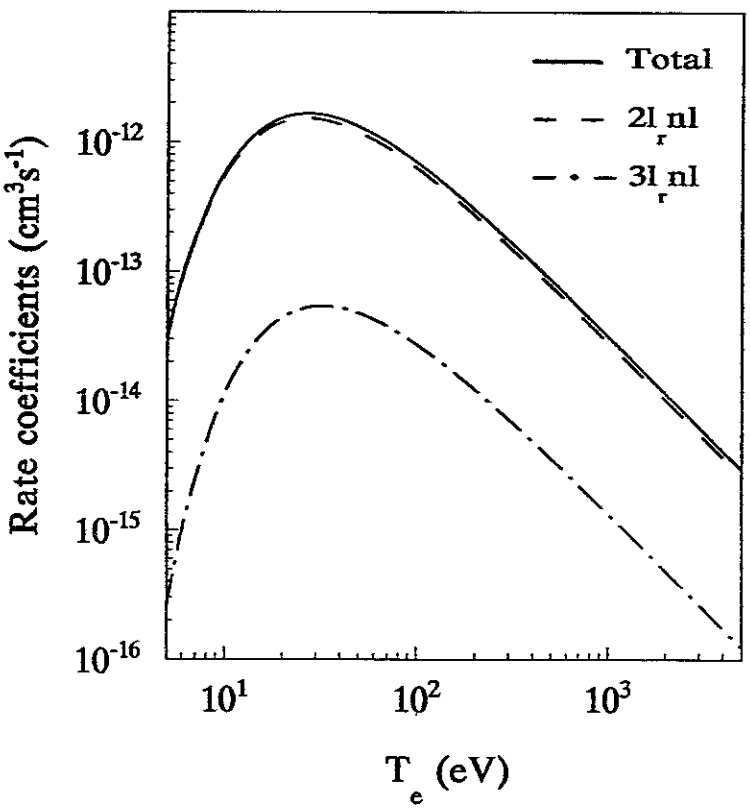

Fig.2 DR rate coefficients as a function of temperature.

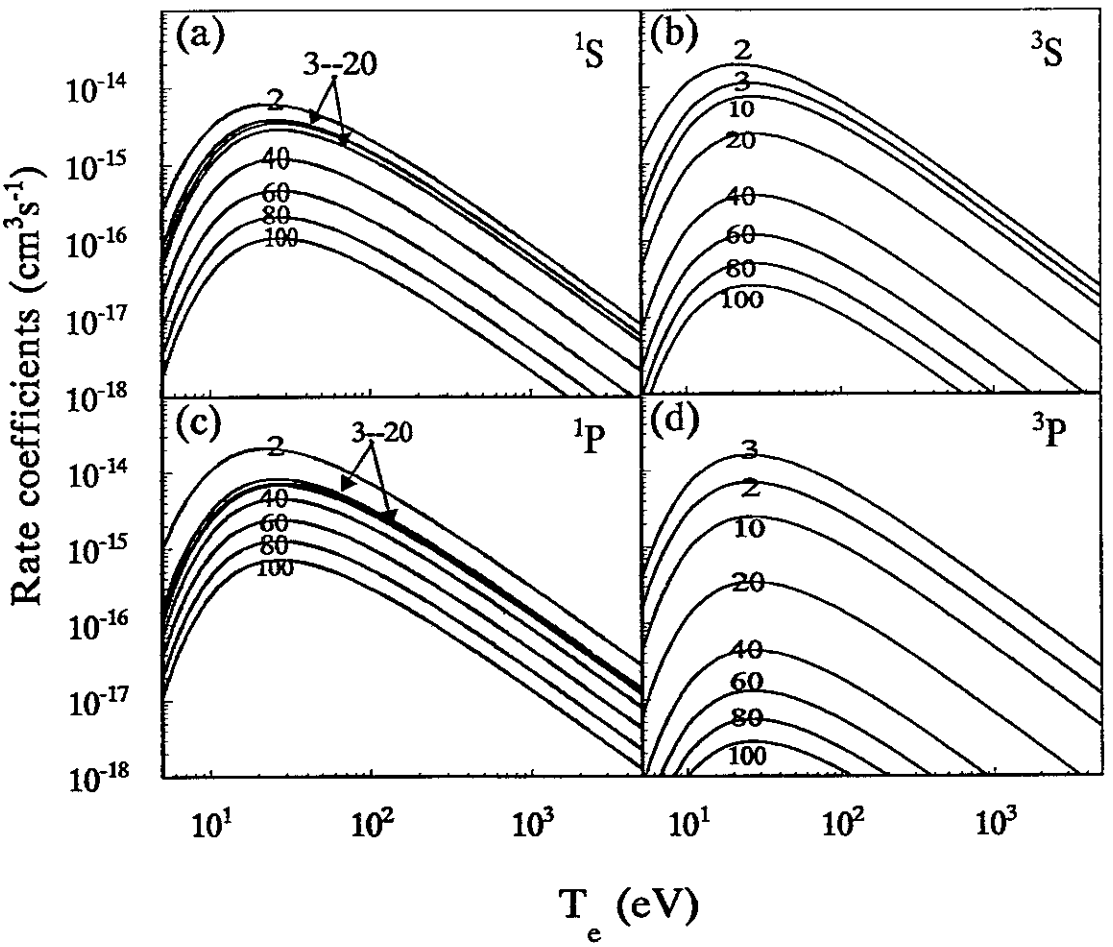

Fig.3 DR rate coefficients to different excited states as a function of temperature. (a). $1sns$ (n^1S); (b). $1sns$ (n^3S); (c). $1snp$ (n^1P); (d). $1snp$ (n^3P)

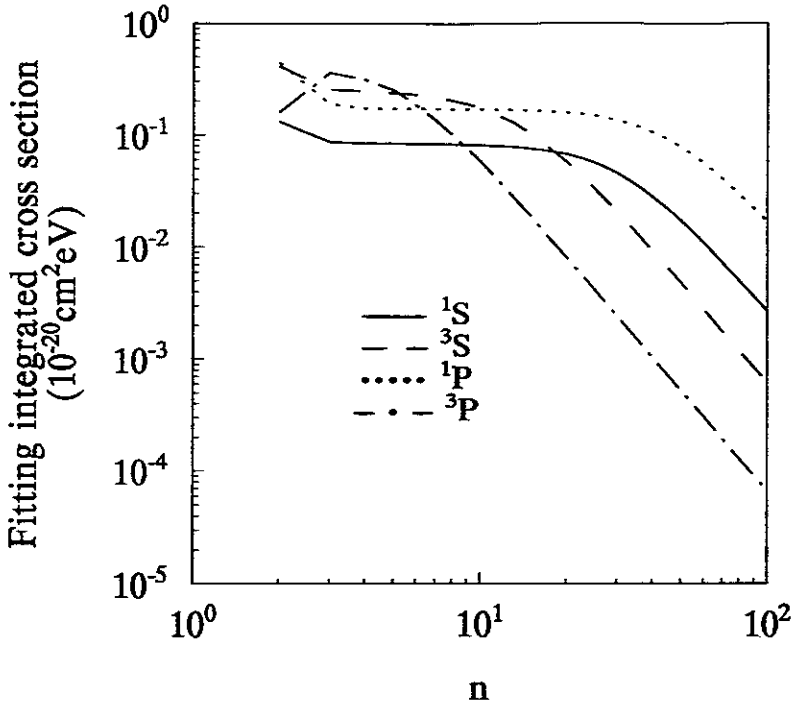

Fig.6 Fitting integrated cross sections as a function of n in different excited states. — : $1sns\ (n^1S)$; - - : $1sns\ (n^3S)$; ··· : $1snp\ (n^1P)$; - · - : $1snp\ (n^3P)$

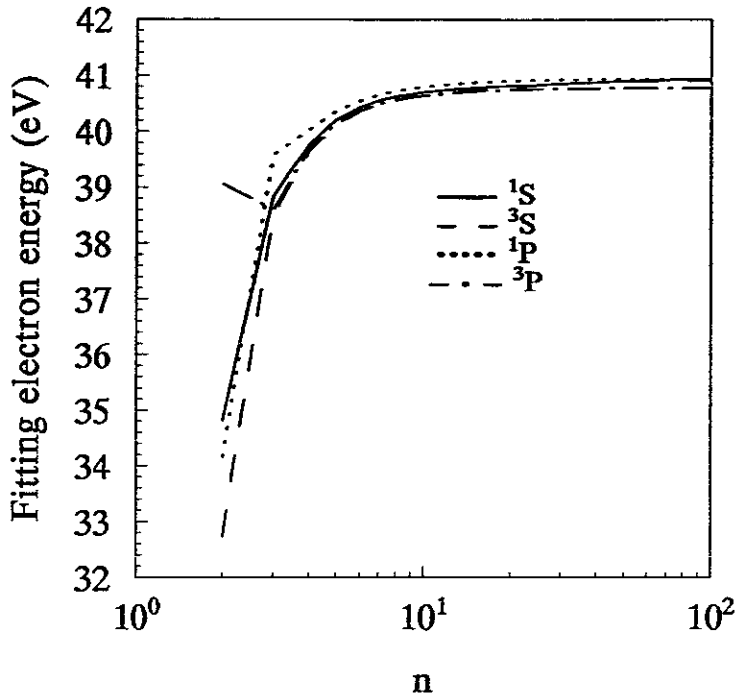

Fig.7 Fitting electron energy as a function of n in different excited states. — : $1sns\ (n^1S)$; - - : $1sns\ (n^3S)$; ··· : $1snp\ (n^1P)$; - · - : $1snp\ (n^3P)$

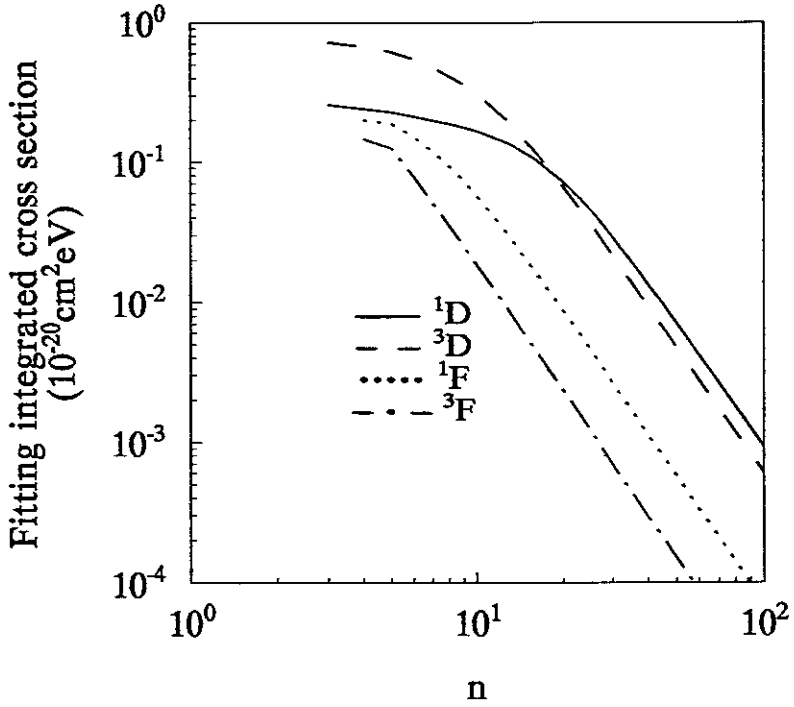

Fig.8 Fitting integrated cross sections as a function of n in different excited states. — : $1snd\ (n^1D)$; - - : $1snd\ (n^3D)$; ··· : $1snf\ (n^1F)$; - · - : $1snf\ (n^3F)$

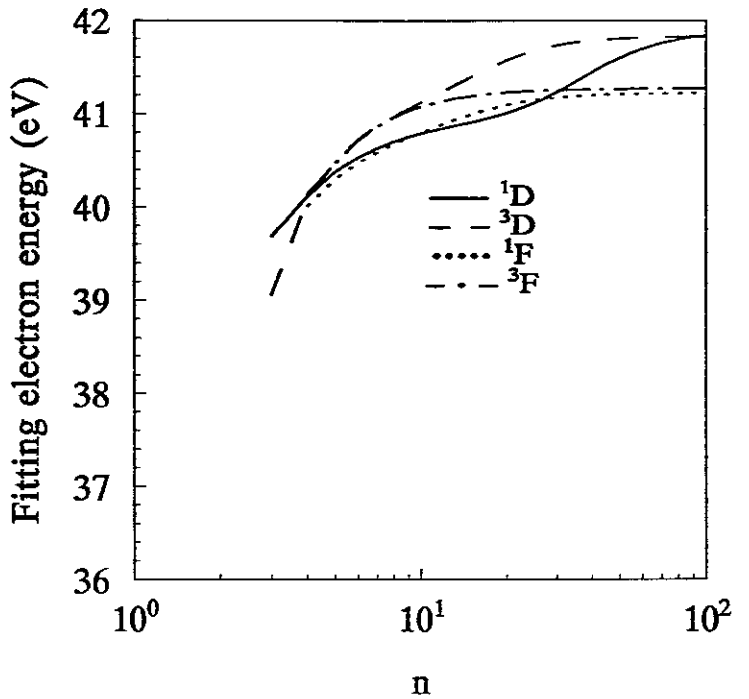

Fig.9 Fitting electron energy as a function of n in different excited states. — : $1snd\ (n^1D)$; - - : $1snd\ (n^3D)$; ··· : $1snf\ (n^1F)$; - · - : $1snf\ (n^3F)$

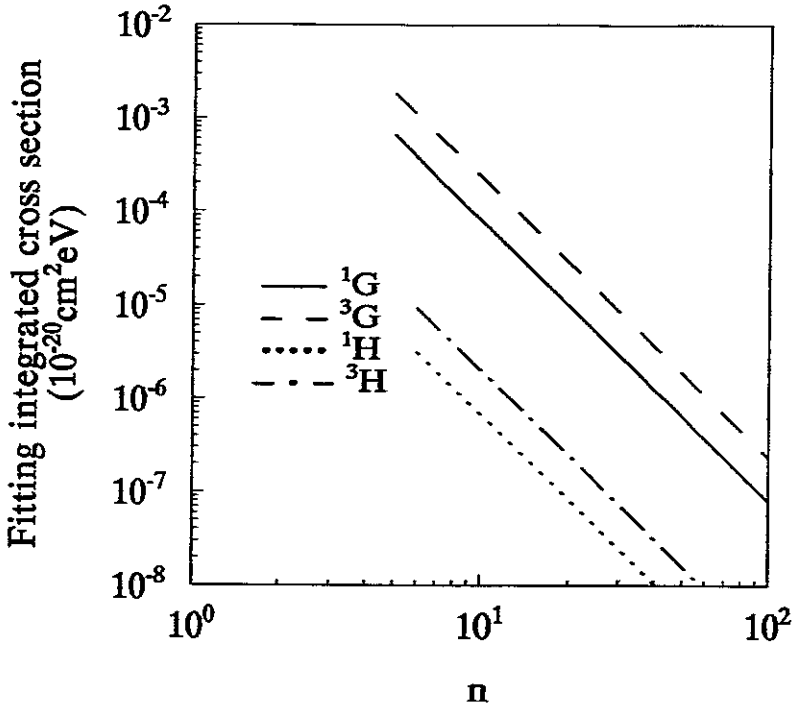

Fig.10 Fitting integrated cross sections as a function of n in different excited states. — : $1sng$ (n^1G); - - : $1sng$ (n^3G); ··· : $1snh$ (n^1H); - · - : $1snh$ (n^3H)

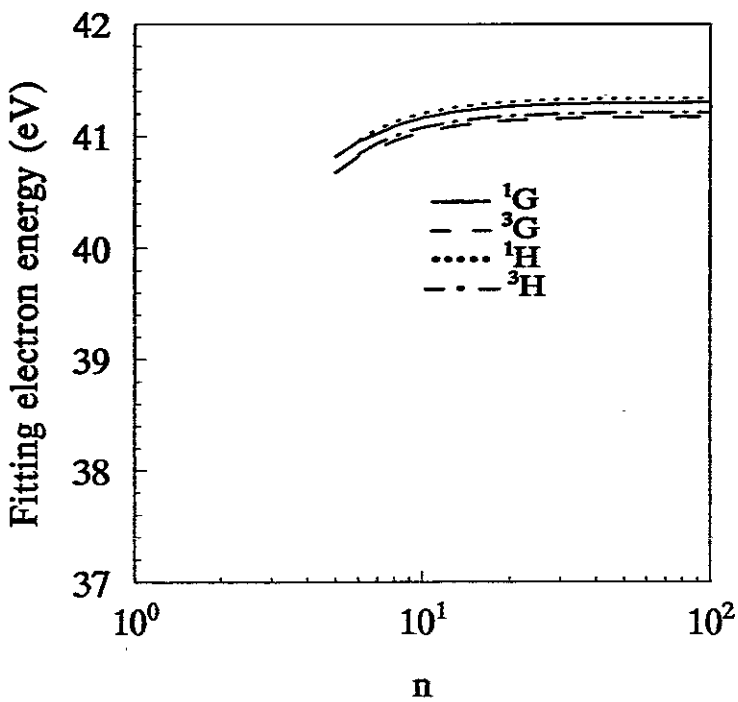

Fig.11 Fitting electron energy as a function of n in different excited states. — : $1sng$ (n^1G); - - : $1sng$ (n^3G); ··· : $1snh$ (n^1H); - · - : $1snh$ (n^3H)

Publication List of NIFS-DATA Series

NIFS-DATA-1 Y. Yamamura, T. Takiguchi and H. Tawara,
Data Compilation of Angular Distributions of Sputtered Atoms; Jan. 1990

NIFS-DATA-2 T. Kato, J Lang and K. E. Berrington,
Intensity Ratios of Emission Lines from OV Ions for Temperature and Density Diagnostics ; Mar. 1990 [At Data and Nucl Data Tables 44(1990)133]

NIFS-DATA-3 T. Kaneko,
Partial Electronic Straggling Cross Sections of Atoms for Protons; Mar. 1990

NIFS-DATA-4 T. Fujimoto, K. Sawada and K. Takahata,
Cross Section for Production of Excited Hydrogen Atoms Following Dissociative Excitation of Molecular Hydrogen by Electron Impact ; Mar. 1990

NIFS-DATA-5 H. Tawara,
Some Electron Detachment Data for H^- Ions in Collisions with Electrons, Ions, Atoms and Molecules – an Alternative Approach to High Energy Neutral Beam Production for Plasma Heating–;Apr. 1990

NIFS-DATA-6 H. Tawara, Y. Itikawa, H. Nishimura, H. Tanaka and Y. Nakamura,
Collision Data Involving Hydro-Carbon Molecules ; July 1990 [Supplement to Nucl. Fusion 2(1992)25; Atomic and Molecular Processes in Magnetic Fusion Edge Plasmas (Plenum, 1995) p461]

NIFS-DATA-7 H.Tawara,
Bibliography on Electron Transfer Processes in Ion-Ion/Atom/Molecule Collisions –Updated 1990–; Aug. 1990

NIFS-DATA-8 U.I.Safronova, T.Kato, K.Masai, L.A.Vainshtein and A.S.Shlyapzeva,
Excitation Collision Strengths, Cross Sections and Rate Coefficients for OV, SiXI, FeXXIII, MoXXXIX by Electron Impact ($1s^22s^2$ -$1s^22s2p$-$1s^22p^2$ Transitions) Dec.1990

NIFS-DATA-9 T.Kaneko,
Partial and Total Electronic Stopping Cross Sections of Atoms and Solids for Protons; Dec. 1990

NIFS-DATA-10 K.Shima, N.Kuno, M.Yamanouchi and H.Tawara,
Equilibrium Charge Fraction of Ions of Z=4-92 (0.02-6 MeV/u) and Z=4-20 (Up to 40 MeV/u) Emerging from a Carbon Foil; Jan.1991 [AT.Data and Nucl. Data Tables 51(1992)173]

NIFS-DATA-11 T. Kaneko, T. Nishihara, T. Taguchi, K. Nakagawa, M. Murakami, M. Hosono, S. Matsushita, K. Hayase, M.Moriya, Y.Matsukuma, K.Miura and Hiro Tawara,
Partial and Total Electronic StoppingCross Sections of Atoms for a Singly Charged Helium Ion: Part I; Mar. 1991

NIFS-DATA-12 Hiro Tawara,
Total and Partial Cross Sections of Electron Transfer Processes for Be^{q+} and B^{q+} Ions in Collisions with H, H_2 and He Gas Targets -Status in 1991-; June 1991

NIFS-DATA-13 T. Kaneko, M. Nishikori, N. Yamato, T. Fukushima, T. Fujikawa, S. Fujita, K. Miki, Y. Mitsunobu, K. Yasuhara, H. Yoshida and Hiro Tawara,
Partial and Total Electronic Stopping Cross Sections of Atoms for a Singly Charged Helium Ion : Part II; Aug. 1991

NIFS-DATA-14 T. Kato, K. Masai and M. Arnaud,
Comparison of Ionization Rate Coefficients of Ions from Hydrogen through Nickel ; Sep. 1991

NIFS-DATA-15 T. Kato, Y. Itikawa and K. Sakimoto,
Compilation of Excitation Cross Sections for He Atoms by Electron Impact; Mar. 1992

NIFS-DATA-16 T. Fujimoto, F. Koike, K. Sakimoto, R. Okasaka, K. Kawasaki, K. Takiyama, T. Oda and T. Kato,
Atomic Processes Relevant to Polarization Plasma Spectroscopy ; Apr. 1992

NIFS-DATA-17 H. Tawara,

Electron Stripping Cross Sections for Light Impurity Ions in Colliding with Atomic Hydrogens Relevant to Fusion Research; Apr. 1992

NIFS-DATA-18 T. Kato,
Electron Impact Excitation Cross Sections and Effective Collision Strengths of N Atom and N-Like Ions -A Review of Available Data and Recommendations- ; Sep. 1992 [Atomic Data and Nuclear Data Tables, 57, 181-214 (1994)]

NIFS-DATA-19 Hiro Tawara,
Atomic and Molecular Data for H_2O, CO & CO_2 Relevant to Edge Plasma Impurities, Oct. 1992

NIFS-DATA-20 Hiro. Tawara,
Bibliography on Electron Transfer Processes in Ion-Ion/Atom/Molecule Collisions -Updated 1993-; Apr. 1993

NIFS-DATA-21 J. Dubau and T. Kato,
Dielectronic Recombination Rate Coefficients to the Excited States of C I from C II; Aug. 1994

NIFS-DATA-22 T. Kawamura, T. Ono, Y. Yamamura,
Simulation Calculations of Physical Sputtering and Reflection Coefficient of Plasma-Irradiated Carbon Surface; Aug. 1994 [J. Nucl. Mater., 220 (1995) 1010]

NIFS-DATA-23 Y. Yamamura and H. Tawara,
Energy Dependence of Ion-Induced Sputtering Yields from Monoatomic Solids at Normal Incidence; Mar. 1995 [At. Data and Nucl. Data Tables, 62 (1996) 149]

NIFS-DATA-24 T. Kato, U. Safronova, A. Shlyaptseva, M. Cornille, J. Dubau,
Comparison of the Satellite Lines of H-like and He-like Spectra; Apr. 1995 [Atomic Data and Nuclear Data Tables, 67., 225 (1997)]

NIFS-DATA-25 H. Tawara,
Roles of Atomic and Molecular Processes in Fusion Plasma Researches - from the cradle (plasma production) to the grave (after-burning) -; May 1995

NIFS-DATA-26 N. Toshima and H. Tawara
Excitation, Ionization, and Electron Capture Cross Sections of Atomic Hydrogen in Collisions with Multiply Charged Ions; July 1995

NIFS-DATA-27 V.P. Shevelko, H. Tawara and E.Salzborn,
Multiple-Ionization Cross Sections of Atoms and Positive Ions by Electron Impact; July 1995 [Suppl. Nucl. Fusion, 6 (1996) 101]

NIFS-DATA-28 V.P. Shevelko and H. Tawara,
Cross Sections for Electron-Impact Induced Transitions Between Excited States in He: n, n'=2,3 and 4; Aug. 1995 [Suppl. Nucl. Fusion, 6 (1996) 27]

NIFS-DATA-29 U.I. Safronova, M.S. Safronova and T. Kato,
Cross Sections and Rate Coefficients for Excitation of $\Delta n = 1$ Transitions in Li-like Ions with $6<Z<42$; Sep. 1995 [Physica Scripta, 54, 68-84 (1996)]

NIFS-DATA-30 T. Nishikawa, T. Kawachi, K. Nishihara and T. Fujimoto,
Recommended Atomic Data for Collisional-Radiative Model of Li-like Ions and Gain Calculation for Li-like Al Ions in the Recombining Plasma; Sep. 1995

NIFS-DATA-31 Y. Yamamura, K. Sakaoka and H. Tawara,
Computer Simulation and Data Compilation of Sputtering Yield by Hydrogen Isotopes ($^1H^+$, $^2D^+$, $^3T^+$) and Helium ($^4He^+$) Ion Impact from Monatomic Solids at Normal Incidence; Oct. 1995

NIFS-DATA-32 T. Kato, U. Safronova and M. Ohira,
Dielectronic Recombination Rate Coefficients to the Excited States of CII from CIII; Feb. 1996 [Physica Scripta, 53, 461-472 (1996), Physica Scripta, 55, 185-199 (1997)]

NIFS-DATA-33 K.J. Snowdon and H. Tawara,
Low Energy Molecule-Surface Interaction Processes of Relevance to Next-Generation Fusion Devices;

Mar. 1996 [Comm. At. Mol Opt. Phys. 34 (1998) 21]

NIFS-DATA-34 T. Ono, T. Kawamura, K. Ishii and Y. Yamamura,
Sputtering Yield Formula for B_4C Irradiated with Monoenergetic Ions at Normal Incidence; Apr. 1996 [J. Nucl. Mater., 232 (1996) 52]

NIFS-DATA-35 I. Murakami, T. Kato and J. Dubau,
UV and X-Ray Spectral Lines of Be-Like Fe Ion for Plasma Diagnostics; Apr. 1996 [Physica Scripta, 54, 463-470 (1996)]

NIFS-DATA-36 K Moribayashi and T. Kato,
Dielectronic Recombination of Be-like Fe Ion; Apr. 1996 [Physca Scripta. Vol.55, 286-297 (1997)]

NIFS-DATA-37 U. Safronova, T. Kato and M. Ohira,
Dielectronic Recombination Rate Coefficients to the Excited States of CIII from CIV; July 1996 [J. Quant. Spectrosc. Radiat. Transfer, 58, 193 - 215, (1997)]

NIFS-DATA-38 T. Fujimoto, H. Sahara, G. Csanak and S. Grabbe,
Atomic States and Collisional Relaxation in Plasma Polarization Spectroscopy: Axially Symmetric Case; Oct. 1996

NIFS-DATA-39 H. Tawara (Ed.)
Present Status on Atomic and Molecular Data Relevant to Fusion Plasma Diagnostics and Modeling; Jan. 1997

NIFS-DATA-40 Inga Yu. Tolstikhina,
LS-Averaged 1/Z Method as a Tool of Studying the Interactions of Highly Charged Ions with a Metal Surface; Jan. 1997

NIFS-DATA-41 K. Moribayashi and T. Kato,
Atomic Nuclear Charge Scaling for Dielectronic Recombination to Be-like Ions; Apr. 1997

NIFS-DATA-42 H. Tawara,
Bibliography on Electron Transfer Processes in Ion-ion / Atom / Molecule Collisions -Updated 1997 -; May 1997

NIFS-DATA-43 M. Goto and T. Fujimoto,
Collisional-radiative Model for Neutral Helium in Plasma: Excitation Cross Section and Singlet-triplet Wavefunction Mixing; Oct. 1997

NIFS-DATA-44 J. Dubau, T. Kato and U.I. Safronova,
Dielectronic Recombination Rate Coefficients to the Excited States of CI From CII;Jan. 1998

NIFS-DATA-45 Y. Yamamura, W. Takeuchi and T. Kawamura,
The Screening Length of Interatomic Potential in Atomic Collisions; Mar. 1998

NIFS-DATA-46 T. Kenmotsu, T. Kawamura, T. Ono and Y. Yamamura,
Dynamical Simulation for Sputtering of B4C; Mar. 1998

NIFS-DATA-47 I. Murakami, K. Moribayashi and T. Kato,
Effect of Recombination Processes on FeXXIII Line Intensities; May 1998

NIFS-DATA-48 Zhijie Li, T. Kenmotsu, T. Kawamura, T. Ono and Y. Yamamura,
Sputtering Yield Calculations Using an Interatomic Potential with the Shell Effect and a New Local Model; Oct. 1998

NIFS-DATA-49 S. Sasaki, M. Goto, T. Kato and S. Takamura,
Line Intensity Ratios of Helium Atom in an Ionizing Plasma;Oct. 1998

NIFS-DATA-50 I. Murakami, T. Kato and U. Safronova,
Spectral Line Intensities of NeVII for Non-equilibrium Ionization Plasma Including Dielectronic Recombination Processses; Jan. 1999

NIFS-DATA-51 Hiro Tawara and Masa Kato,
Electron Impact Ionization Data for Atoms and Ions -up-dated in 1998-;Feb. 1999

NIFS-DATA-52 J.G. Wang, T. Kato and I. Murakami,
Validity of n^{-3} Scaling Law in Dielectronic Recombination Processes; Apr. 1999

NIFS-DATA-53 J.G. Wang, T. Kato and I. Murakami,
Dielectronic Recombination Rate Coefficients to Excited States of He from He^{+}; Apr. 1999